**TITLE**
ASP Conference Series, Vol. **VOLUME**, **PUBLICATION YEAR**
**EDITORS**

# Atmospheric Turbulence Profiles $C_n^2(h)$ deduced from Solar Limb Observations

Bouzid A., Irbah A.

*C.R.A.A.G - Observatoire d'Alger BP 63 Bouzaréah Alger Algérie*

Borgnino J. & Lantéri H.

*Université de Nice-Sophia Antipolis, UMR 6525 Astrophysique, Parc Valrose F-06108 Nice Cedex 2 France*

**Abstract.** Atmospheric turbulence is responsible of the spatio-temporal fluctuations in astronomical object images obtained by means of ground-based telescopes. They are due to wave-front degradations present at the entrance of the instrument pupil plane. We first establish in this paper the formulation of the angle-of-arrival angular structure function $d(\theta)$ of image fluctuations which is linked to the turbulence "optical strength" $C_n^2(h)$. We use this property to propose an optical method to estimate atmospheric turbulence profiles. This is based on the inversion of the $d(\theta)$ integral equation using the Marquardt-Levenberg method. Application to synthetic data shows the efficiency and the stability of the developed method. We applied then this method to estimate optical turbulence profiles from the analysis of solar limb images.

## 1. Introduction

The terrestrial atmosphere is widely responsible of the degradations observed on the images recorded with a ground-based telescope. These degradations are more or less important according to the Earth turbulence state in the line of sight at the moment of the observations. In fact, the wave-fronts coming from a point source through the atmospheric turbulent layers are randomly perturbed in space and time which gives a random behavior of the point spread function of the whole atmosphere-telescope system . The knowledge of the vertical localization of the turbulence "optical strength" $C_n^2(h)$ (structure constant of the air-refractive-index fluctuations) is fundamental in adaptive optics since it defines the isoplanatic patch (Molodji & Rousset 1997) and the magnitude of the focus anisoplanatism effect when laser guide stars are used (Fried & Belsher 1994). In addition, the localization of the turbulent layers allows the use of multiconjugate adaptive optics in order to correct for low and high altitude contributions to atmospheric distortion on images (Johnston & Welsh 1994, Beckers 1988). The knowledge of this parameter gives also access to the quality of the observations (Fried's parameter $r_0$ Fried 1966, Irbah et al. 1993) and to the optical transfer function (Roddier 1981).
The aim of this paper is to present an optical method leading to estimations of

the turbulence profiles from extended object observations. We first establish the expressions of the angular covariance and the structure function for the $AA$ fluctuations. We present in the next section the inversion method used to process, in a first time, synthetic profile models. It is then applied to solar data in order to estimate profile for daytime observations. The first experimental results are presented in the last section and discussed.

## 2. Angle of Arrival angular covariance and structure function

Let $\alpha(\overrightarrow{r}, t, \overrightarrow{\eta})$ the $AA$ fluctuations observed at the $\overrightarrow{r}$-position of the perturbed wavefront, at the t-time and in the $\overrightarrow{\eta}$-direction (Figure 1). They are assumed to be described by a stationary and homogeneous random process. When the observations are performed simultaneously in two angular directions $\overrightarrow{\eta}$ and $\overrightarrow{\eta} + \overrightarrow{\theta}$, the spatio-angular covariance of these fluctuations for two positions separated by a baseline $\overrightarrow{B}$ is :

$$\mathcal{C}_{\alpha,\overrightarrow{B}}(\theta) = < \alpha(\overrightarrow{r}, t, \overrightarrow{\eta})\alpha(\overrightarrow{r} + \overrightarrow{B}, t, \overrightarrow{\eta} + \overrightarrow{\theta}) > \quad (1)$$

where $<>$ symbolizes an ensemble average. We consider now a turbulent layer at the altitude $h$. The $AA$ fluctuations observed in the angular direction $\overrightarrow{\eta} + \overrightarrow{\theta}$ may be described by :

$$\alpha(\overrightarrow{r} + \overrightarrow{B}, t, \overrightarrow{\eta} + \overrightarrow{\theta}) = \alpha(\overrightarrow{r} + \overrightarrow{B} - \overrightarrow{\theta}h, t, \overrightarrow{\eta}) \quad (2)$$

and the spatio-angular covariance is related to the spatial covariance $C$ by :

$$\mathcal{C}_{\alpha,\overrightarrow{B}}(\theta) = C_{\alpha,\overrightarrow{B}}(\overrightarrow{\theta}h - \overrightarrow{B}) \quad (3)$$

Since the $AA$ fluctuations are observed in the direction perpendicular to the baseline, the transverse spatio-angular covariance is given by (Avila et al. 1997):

$$\mathcal{C}_{\alpha,\overrightarrow{B}}(\theta) = 0.0716\lambda^2 r_0^{-\frac{5}{3}} \int_0^{+\infty} df f^3 (f^2 + \frac{1}{L_0^2})^{-\frac{11}{6}}$$
$$[J_0(2\pi f(\theta h - B)) + J_2(2\pi f(\theta h - B))][\frac{2J_1(\pi D f)}{\pi D f}]^2 \quad (4)$$

where $\theta$ and $B$ are respectively the modulus of $\overrightarrow{\theta}$ and $\overrightarrow{B}$. The model in use is the so-called Von Kàrmàn model, $\lambda$, $r_0$, $L_0$ and $D$ are respectively the light wavelength, the Fried parameter, the spatial coherence outer scale and the pupil diameter. The wavefront inner scale $l_0$ is assumed to be equal to 0 and the angular direction $\overrightarrow{\theta}$ is assumed to be the same that the one of the baseline $\overrightarrow{B}$. Doing $B = 0$ in equation (4) and in the case of a multilayer situation, the $AA$ angular covariance becomes :

$$\mathcal{C}_{\alpha,0}(\theta) = 1.19 \int_0^{+\infty} dh C_n^2(h) \int_0^{+\infty} df f^3 (f^2 + \frac{1}{L_0(h)^2})^{-\frac{11}{6}}$$
$$[J_0(2\pi f\theta h) + J_2(2\pi f\theta h)][\frac{2J_1(\pi D f)}{\pi D f}]^2 \quad (5)$$

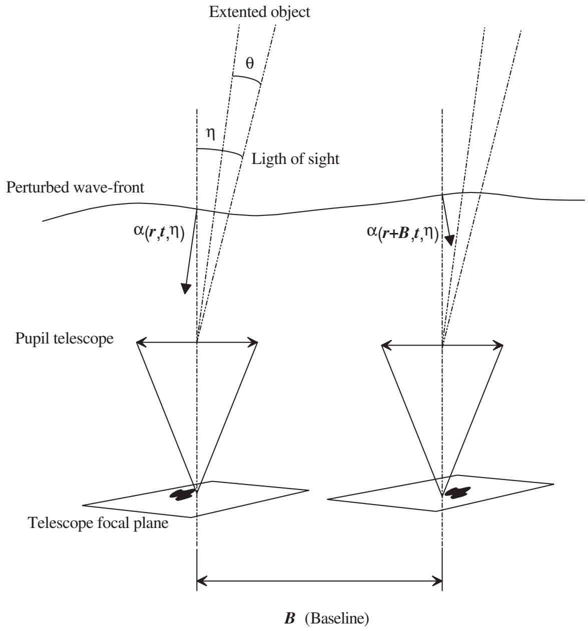


Figure 1. Used notations to characterize the perturbed wave-front

where $C_n^2(h)$ is the energy vertical profile of the " optical " turbulence given by the structure constant for the air refractive index fluctuations and $L_0(h)$ is the turbulent outer scale vertical profile.
The transverse angular structure function is given by :

$$d_\alpha(\theta) = 2[\sigma_\alpha^2 - \mathcal{C}_{\alpha,0}(\theta)] \tag{6}$$

where $\sigma_\alpha^2 = C_{\alpha,0}(0)$. Introducing (5) in equation (6) leads to :

$$d_\alpha(\theta) = 2.4 \int_0^{+\infty} dh C_n^2(h) \int_0^{+\infty} df f^3 (f^2 + \frac{1}{L_0(h)^2})^{-\frac{11}{6}}$$
$$[1 - J_0(2\pi f \theta h) - J_2(2\pi f \theta h)][\frac{2J_1(\pi D f)}{\pi D f}]^2 \tag{7}$$

In this work, we are interested by the atmospheric turbulence profile and, therefore, we consider the case in which $L_0(h) = \infty$.

## 3. Estimation of the atmospheric turbulence profile from the *AA* fluctuations

### 3.1. The inversion method

Equation (7) shows that the angular structure function $d_\alpha(\theta)$ is linked to the turbulence "optical strength" $C_n^2(h)$ by a Fredholm integral equation of the first kind. It can be wrote as following (in seek of simplicity, the $\alpha$ index is removed from $d_\alpha(\theta)$ hereafter)

$$d(\theta) = \int_0^{+\infty} dh C_n^2(h) k(h,\theta,D) \tag{8}$$

where $k(h,\theta,D)$ is the integral's kernel given by

$$k(h,\theta,D) = 2.4 \int_0^{+\infty} df f^{-\frac{2}{3}} [1 - J_0(2\pi f\theta h) - J_2(2\pi f\theta h)][\frac{2J_1(\pi Df)}{\pi Df}]^2 \tag{9}$$

The integrand goes to zero when $f$ increases but does not vanish in the $h$ variation range corresponding to the atmosphere thickness affecting the optical observations. If we assume that the atmosphere is formed by a stratification of $N$ layers where $C_n^2(h)$ is constant within each layer and equal to zero elsewhere, equation (8) can be wrote under the following matrix form :

$$d = K.C \tag{10}$$

where $d$ is a $M$ x 1 vector of the angular structure function, $K$ is a $M$ x $N$ matrix which depends only on the discretization of observation ($\theta$) and parameter($h$) spaces, and $C$ is a $N$ x 1 vector representing the atmospheric turbulence profile. In Figure 2, $K$ is plotted for a fixed value of the pupil diameter $D$ equal to 10 cm, for $0 < h < 30$ km and $0 < \theta < 128$ arcseconds, which are typical values of $h$ and $\theta$. For all values of $\theta$, $K$ increases with the altitude and therefore, the highest turbulent layers contribute to the observed angular structure function more than the lowest ones. Estimate the atmospheric turbulence profile $C$ from the observed angular structure function is a linear but ill-posed problem in the sense that small changes in the data lead to large changes in the solution (Jupp & Vozoff 1975). Figure 2 shows also the singular values of $K$ calibrated by the greatest one ($s_1$). $K$ is calculated for an atmosphere descritized on 30 layers over 30 km thick. The small singular values are corrupted by machine zeroing and show the fact that $K$ is ill-conditioned ($s_{30}/s_1 \approx 10^{-10}$). Furthermore, the inverse of $K$ amplifies the noise in data which affects the solution. To estimate the turbulence profile from the observed $d(\theta)$, the Marquardt-Levenberg method was used (Marquardt 1963, Levenberg 1944, Bouzid et al. 1999). It consists to solve the system :

$$\delta d = K.\delta C \tag{11}$$

which is obtained by transforming equation (10) and by minimizing the functional :

$$\phi = \|\delta d - K.\delta C\|^2 + \nu^2 \|\delta C\|^2 \tag{12}$$

with respect to $\delta C$. Here $\delta d = d - d_0$, $\delta C = C - C_0$, $C_0$ is the first estimate of $C$ and $\nu$ is the Marquardt parameter (Jupp & Vozoff 1975).
Minimizing the functional $\phi$ leads to the solution :

$$\delta C = (K^T.K + \nu^2.I)^{-1}.K^T.\delta d \tag{13}$$

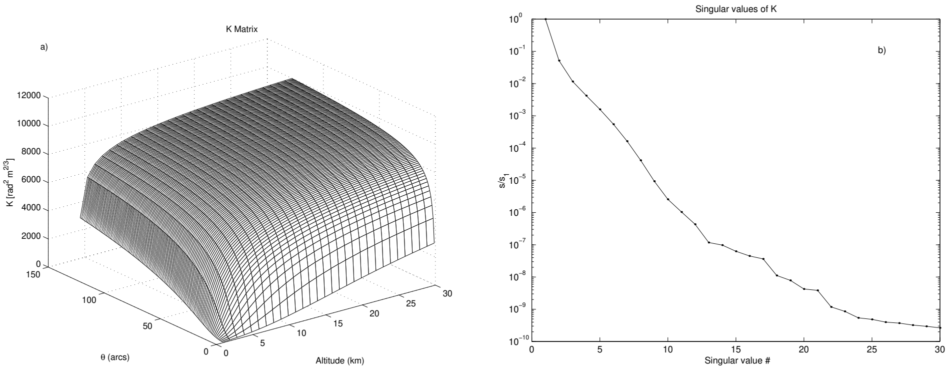


Figure 2. a) $K$ matrix. b): Singular values $s_i$ of $K$.

At iteration $k+1$ :

$$C_{k+1} = C_k + (K^T.K + \nu^2.I)^{-1}.K^T.(d_{obs} - K.C_k) \quad (14)$$

Finally, to get a stable solution, all variables are rescalled as (Neumaier 1998)

$$C_{k+1} = C_k + L_C.(K'^T.K' + \nu^2.I)^{-1}.K'^T.(L_d^{-1}.d_{obs} - K'.L_C^{-1}.C_k) \quad (15)$$

where $L_d = diag(d)$, $L_C = diag(C)$ and $K' = L_d^{-1}.K.L_C$. Thus, this makes $K'$ dimension free and makes the problem more stable. To initialize the later iterative process, a first estimate ($C_0$) is calculated by solving the equation (10) in least-square sense. To get a stable solution, one minimizes :

$$L = \|d_{obs} - K.C\|^2 + \gamma\|C\|^2 \quad (16)$$

with respect to the vector parameter $C$. This leads to the solution :

$$C_0 = (K^T.K + \gamma I)^{-1}.K^T.d_{obs} \quad (17)$$

$\gamma$ is used to stabilize and smooth the solution.

### 3.2. Application on synthetic data

Applications on synthetic data are performed to study the efficiency, the robustness of the inverse method developed in previous subsection and the data noise effect on the solution. Two atmospheric turbulent profiles were used: (1) a two-layer profile with a lower layer of 1 km thick and an upper one located between altitudes 4 and 6 km (figure 3a) and (2) the Hufnagel mean turbulent profile for day-time observations (figure 3b). For both profiles angular structure function $d_i^{noisefree}$ is generated using the forward formula (equation (10)) to which noise was added. For an angle $\theta_i$, noisy $d_i$ is calculated as :

$$d_i = d_i^{noisefree} + n_i \quad (18)$$

$n_i$ is calculated from a normal distribution with mean equal to $d_i^{noisefree}$ and standard deviation equal to a percentage of $d_i^{noisefree}$. Figure 3 shows synthetic

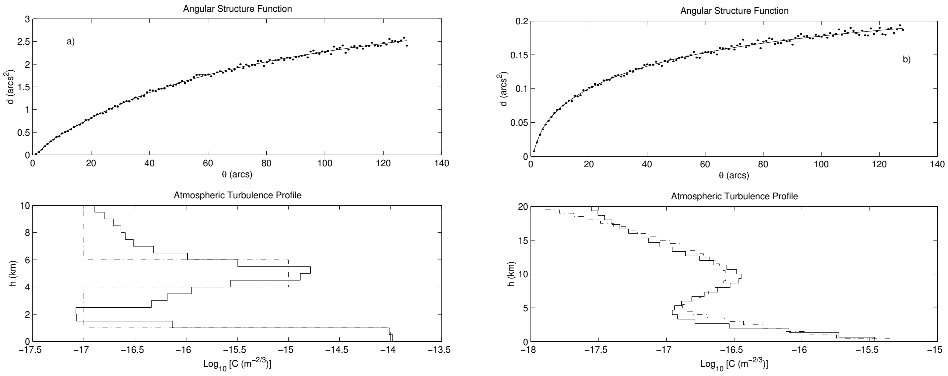


Figure 3. Reconstruction of synthetic atmospheric turbulence profiles. a) two-turbulent layers profile. At the top: fit between the synthetic noisy data (dot) and the predicted structure function (solid line). At the bottom: solution obtained (solid line) by comparison to the theoretical profile (dashed line). b)The Hufnagel mean profile (same notation).

data with a 2% standard deviation about a noise-free data (noise level of 2%). The synthetic data obtained were inverted according to the developed method. The algorithm converges in a few iterations and a satisfactory solution is found. In the two synthetic data sets, the turbulent layers are well restored and their altitude is resolved. However, the turbulent layers located near the ground are well reconstructed than the higher ones which need some additional iterations to reconstruct them. Moreover, these higher layers are more sensitive to the noise in data. Thus, if the noise level is high the threshold $\nu$ should be increased to avoid numerical instabilities but, unfortunately, this makes difficulties to restore the highest turbulent layers. Applications on synthetic data show that the method works efficiently if the problem is well parameterized. That is the appropriate number of layers, the thickness of the considered terrestrial atmosphere and threshold values must be well selected. A few layer model leads to stable inverse but can not resolve thin layers. In the opposite, when the layer number is chosen very large in order to resolve thin layers, it causes numerical instabilities in the solution. Between these extreme limits, an appropriate number of layers should be found which allows to recover the fine features of the solution without instabilities. The same problem occurs with the choice of the threshold $\nu$: a compromise should be found between a large value that leads to stable but very smooth solution without fine features and very small one, which produces instabilities in the solution. Applications on synthetic data shows that the best strategy is to start with large value of the threshold to obtain the mean features of the solution and decrease the $\nu$ value with the iterations to get details in the solution.

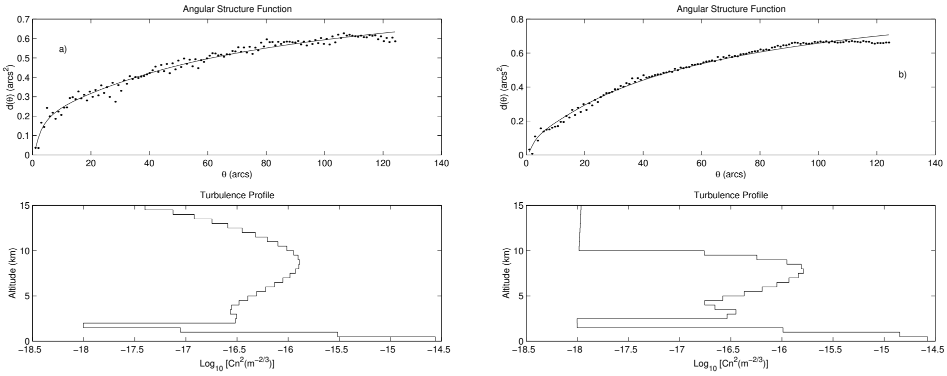


Figure 4. Estimation of atmospheric turbulence profile from real data. (a) at the top: data set1 (.) and the fit deduced from the solution (-). At the bottom: the obtained solution . (b) data set2 (same notation)

## 4. Applications on real data obtained from solar image analysis

In this section the inverse method is applied to real data obtained from the analysis of solar images. Two sets of day-time observations are used to estimate the atmospheric turbulence profile. Each data set consist in a sequence of 128 short exposure time image frames of 8 ms. These observations have been performed during the same day in June 1990 at the solar astrolabe of the Calern Observatory (Observatoire de la Côte d'Azur, France). The instrument has an elliptic objective with major axis equal to 8 cm and the minor one equal to 5 cm. The data show an angular structure function highly corrupted by noise. These two data sets are inverted according to the method developed above. A discretization on 30 layers of equal thickness over an atmosphere of 15 km thick was used. The solution obtained shows an atmospheric turbulence profile dominated by two turbulent layers. A strong turbulent layer is located at the atmosphere bottom. The second layer is located at 8.5 km high (Figure 4a). Unfortunately, the thickness of these two turbulent layers can not be well resolved. The lower layer needs more fine discretization to be resolved but this lead to unstable solution. The higher one is smoothed by the constraint adopted using the Marquardt-Levenberg method. The calculated Fried parameter from the atmospheric turbulence profile estimated is $r_0 = 5.0cm$ $(\lambda = 0.55\,10^{-6}m)$.The same discretization was used to invert the second data set. The solution obtained by inversion exhibits mainly two turbulent layers (Figure 4b). A lower layer with strong value of energy and a second one located at 8.0 km high. The estimated Fried parameter for this atmospheric profile is $r_0 = 4.6$ cm.

## 5. Conclusion

An integral expression was established, in the framework of the Von Kàrmàn turbulence model, that links the angle-of-arrival angular structure function to the atmospheric turbulence profile along an optical path. As a first approach, the case $L_0 = \infty$ was considered. This integral equation allows to estimate the atmospheric turbulence profile from the structure function extracted from solar limb images. This later operation is an ill-posed inverse problem despite the fact that it is linear in $C_n^2(h)$. The Marquardt-Levenberg method was used and allows to get a smooth and stable solution. Application to real data recorded at Calern Observatory (France) shows a good results in accordance with other results obtained at the same site.

**Acknowledgments.** This work has been performed with support of the Observatoire d'Alger (C.R.A.A.G), the Algerian National Research Program (PNR) and the French Foreign Affair Ministry in the framework of scientific cooperation between France and Algeria (contract 00 MDU 501)

## References

Aime, C., Borgnino, J., Martin, F., Petrov, R., Ricord, J. & Kadiri, S. 1986, J. Opt. Soc. Am., 3, 7, 1001

Avila, R., Ziad, A., Borgnino, J., Martin, F., Agabi, A., & Tokovinin, A. 1997, J. Opt. Soc. Am. A,14(11), 3070

Borgnino, J. 1990, Appl.Optics, 29, 13, 1863

Bouzid, A. et al. 1999, in ESA SP-437, 453

Beckers, J. M. 1988,in Very Large Telescopes and their Instrumentation, M. H. Ulrich ed., European Southern Observatory Proceedings N30, (European Southern Observatory Garching bei München, Germany), 693

Fried, D. L. 1966, J. Opt. Soc. Am., 56, 1372

Fried, D. L. & Belsher, J. F. 1994, J. Opt. Soc. Am. A, 11, 1, 277

Irbah, A., Borgnino, J., Laclare F. & Merlin, G. 1993, A&A, 276, 663

Johnston, D. C. & Welsh, B. M. 1994, J. Opt. Soc. Am. A, 11, 1, 394

Jupp, D. L. B. & Vozoff, K. 1975, Geoph. J. Roy. Astro. Soc., 42,957

Lanczos, C. 1958, Am. Math. Monthly, 5, 665

Levenberg, K. 1944, Quarterly of Applied Mathematics, 2, 164

Marquardt, D. W. 1963, J. SIAM, 11, 431

Molodij, G. & Rousset, G. 1997, J. Opt. Soc. Am. A, 14, 8, 1949

Neumaier, A. 1998, SIAM Review, 40, 636

Roddier, F. 1981, Progress in Optics, 19, E. Wolf (ed), North-Holland publishing Co, Amsterdam

Roddier, F., Gilli, J. M. & Vernin, J., 1982, J. Opt. (Paris) 13,2, 63

Roddier, F., Gilli, J. M. & Lund, G. 1982, J. Opt. (Paris) 13, 263

Tatarski, V. I. 1971, Israel Program of Scientific Translation, Jerusalem